JOURNAL OF CHEMICAL ENGINEERING AND INDUSTRIAL BIOTECHNOLOGY (JCEIB)
ISSN: 2600-7347 e-ISSN: 0126-8139
VOL. 08, ISSUE 01, 18 – 26
DOI: https://doi.org/10.15282/jceib.v8i1.7774

ORIGINAL ARTICLE

Optimization of Pb(II) Removal using Magnetic γ-Fe_2O_3/KCC-1 Synthesized from Palm Oil Fuel Ash

J. Q. Lim[1], R. S. R. Mohd Zaki[1], S. N. Miskan[1], N. Ainirazali[1,2*], N. F. Jaafar[3]

[1]Faculty of Chemical and Process Engineering Technology, Universiti Malaysia Pahang, 26300 Gambang, Kuantan, Pahang, Malaysia.
[2]Centre for Research in Advanced Fluid & Processes, Universiti Malaysia Pahang, 26300 Gambang, Kuantan, Pahang, Malaysia.
[3]School of Chemical Sciences, Universiti Sains Malaysia, 11800 USM Penang, Malaysia.

ABSTRACT – The pollution of lead, Pb(II) in water bodies has severely threatened the environment and human health due to its toxicity. Thus, removing Pb(II) from water bodies is an imperative task. In this study, the removal of Pb(II) using magnetic γ-Fe_2O_3/KCC-1 synthesized from Palm Oil Fuel Ash (POFA) was explored. The characterization analysis confirmed a successful preparation of γ-Fe_2O_3/KCC-1 with BET surface area and pore volume of 401 m^2g^{-1} and 0.90 cm^3g^{-1}, respectively. The optimization by response surface methodology (RSM) with independent variables of initial Pb(II) concentration (X_1), γ-Fe_2O_3/KCC-1 dosage (X_2), and initial pH (X_3) was performed. The ANOVA analysis exhibited that the most significant parameter was initial Pb(II) concentration. The maximum Pb(II) removal of 91% experimentally and 90.11% predictably were accomplished under optimum conditions (X_1= 302.37 mg/L, X_2 = 2.44 g/L, and X_3 = 5.7). The findings revealed that the magnetic γ-Fe_2O_3/KCC-1 has the potential to serve as an excellent adsorbent for the elimination of Pb(II) from an aqueous solution.

ARTICLE HISTORY
Received: 5 June 2022
Revised: 22 June 2022
Accepted: 30 June 2022

KEYWORDS
KCC-1
Magnetic γ-Fe_2O_3
Adsorption
Pb(II) removal
Optimization

INTRODUCTION

Lead (Pb(II)) is broadly used in many industrial activities, for example, lead-acid battery production, metal recycling, petroleum refining, mining, and smelting [1]. Water pollution caused by Pb(II) has grown into health and environmental problems. Depending on the degree of lead exposure, it may adversely cause the malfunction of the human body system, especially reproductive and developmental systems, cardiovascular system, and immune system, and even reduce the oxygen-carrying capacity of the bloodstream [2]. Babies and kids are particularly sensitive even at a low level of Pb(II) Meanwhile, people with prolonged exposure to a Pb(II) are at a higher risk of kidney disease, heart issues, high blood pressure, and reduced fertility [3]. Hence, the removal of Pb(II) from wastewater is an important task before the water spreads into the open area.

There are several methods have been developed and reported for the removal of Pb(II) ions, such as adsorption [4], ion exchange separation [5], chemical precipitation [6], electrochemical treatment [7], and chemical coagulation [8]. Among all, the adsorption method is chosen to be the most suitable, economical, and frequently used due to its effectiveness, simplicity, and affordable cost [9-10].

In recent years, a unique kind of mesoporous silica material called dendritic fibrous Nano-silica (DFNS), also named KCC-1, has gained considerable attention in multiple applications. This is due to its exceptional physicochemical features, including high surface area, broad pore diameter, fibrous surface morphology, and superior mechanical durability [11]. However, the production cost of this material is relatively high owing to the price of the chemical used. Thus, the idea of preparing the KCC-1 from low-cost silica-rich wastes is an interesting approach.

Numerous silica-rich wastes have been used as an alternative silica source, including rice husk ash (RHA), sugarcane bagasse, fly ash, and palm oil fuel ash (POFA), owing to their high composition of silica content and abundance. Previously, Hasan et al. [12] reported the potential of RHA as a silica source of KCC-1, and the characterization results revealed the comparable properties of the synthesized KCC-1 with the conventional KCC-1. In conjunction with this study, it is desirable to study the potential of POFA in preparing KCC-1 owing to its high composition of silica (57-67%) and abundance [13]. In addition, POFA has shown its potential as an alternative sodium silicate (Na_2SiO_3) for SBA-15 synthesis, as reported in our previously published article [13].

In the meantime, iron oxide (Fe_2O_3) offers various advantages for water treatment applications owing to its small size, high stability, high surface-area-to-volume ratio, and biocompatibility [14]. Fe_2O_3-type adsorbents have been widely employed with impressive adsorption effectiveness approaching 100% for some contaminants. Recently, the magnetic type of Fe_2O_3 (γ-Fe_2O_3) has attracted researchers' attention due to its advantages in better separation for regeneration and reusability [15]. However, γ-Fe_2O_3 tends to aggregate easily, and thus the introduction of support material is needed to ensure homogeneous distribution of γ-Fe_2O_3 for the adsorption process [16]. Hence, in this study, magnetic γ-Fe_2O_3/KCC-1 was prepared as an adsorbent for Pb(II) removal, and the adsorption process was optimized using response surface methodology (RSM).

*CORRESPONDING AUTHOR | N. AiniRazali | ✉ ainirazali@ump.edu.my

MATERIALS AND METHOD

Preparation of magnetic γ-Fe_2O_3/KCC-1

POFA sodium silica solution (Na_2SiO_3-POFA) was prepared according to our previously published article [13] and the amount of SiO_2 in Na_2SiO_3-POFA was 20.16%. KCC-1 was synthesized according to the method described by Hasan et al. [12]. In brief, cetyltriammonium bromide (CTAB, Sigma Aldrich) and urea (Merck) were dissolved in distilled water and agitated for 10 minutes. After 15 minutes, *n*-butanol (Merck) and toluene (Merck) were added to the beaker with continuous stirring. Next, Na_2SiO_3-POFA was added dropwise to the solution, and the mixture was agitated for another 2 hours. The solution was then heated (120 °C, 4 hours) in a Teflon-sealed hydrothermal reactor, followed by centrifuged, filtered, and calcined to obtain KCC-1.

Next, magnetic γ-Fe_2O_3/KCC-1 was prepared by the impregnation method as reported in the literature [17]. 1.0 g of synthesized KCC-1 and 6.0 g of ferric ammonium citrate ($(NH_4)_5[Fe(C_6H_4O_7)_2]$, Sigma Aldrich) were added to 20 mL of distilled water and left overnight. The sediment suspension was filtered, rinsed, dried in an oven (60 °C), and calcined in a furnace for 6 hours at 400 °C.

Characterization of magnetic γ-Fe_2O_3/KCC-1

Transmission Electron Microscopy (TEM, Philips CM12) was utilized to investigate the morphology of γ-Fe_2O_3/KCC-1. Meanwhile, Brunauer-Emmett-Teller (BET, Micromeritics) method was employed to investigate the surface area (*SA*) and total pore volume (V_p) of γ-Fe_2O_3/KCC-1.

Batch Adsorption Experiment

Batch adsorption testing was performed following the experimental design derived from the RSM. The initial Pb(II) concentration, adsorbent dose, and initial pH were chosen as independent variables. Pb(II) solution was made by stirring a measured amount of lead nitrate ($Pb(NO_3)_2$, Sigma Aldrich, 99% purity) in distilled water to achieve the necessary concentration. The pH of the Pb(II) solution was modified according to the desired pH. Then, a specific amount of adsorbent (magnetic γ-Fe_2O_3/KCC-1) was added to the solution, with the mixture being constantly stirred at 200 rpm. At an appropriate time, the samples were withdrawn and analyzed using Ultraviolet-Visible Spectroscopy (UV-Vis) at a wavelength of 520 nm. The amounts of Pb(II) adsorbed at equilibrium, q_e was computed by using Equation (1).

$$q_e = \left(\frac{C_0 - C_e}{m}\right) \times V \tag{1}$$

The percentage removal of Pb(II) was estimated using Equation (2).

$$Removal\ (\%) = \frac{C_0 - C_e}{C_0} \times 100\% \tag{2}$$

Where the q_e represents the quantity of Pb(II) adsorbed at equilibrium (mg/g), V represent the volume (L), m represents the mass of the adsorbent (g), C_0 and C_e represent the liquid-phase concentrations of Pb(II) before and after the adsorption (mg/L), respectively [18].

Experimental Design and Optimization

Statsoft Statistica 10.0 with the face-centered composite design (FCCD) was used to investigate the independent variables of initial Pb(II) concentration (X_1), adsorbent dosage (X_2), and initial pH (X_3). The independent variables were coded to (-1,0,1) interval where the low level was coded by -1, the middle level by 0, and the high level by 1. The whole number of tests that were carried out was 16; 2^3 factorial points, 6 axial points, and 2 replicates at the center points. To ensure reliable data, every experiment was repeated thrice. The parameters and range were selected according to the previous investigation [19]. The prediction of the optimum condition of Pb(II) removal was conducted by analysis of the quadratic model.

RESULTS AND DISCUSSION

Characterization of magnetic γ-Fe_2O_3/KCC-1

Table 1 shows the BET analysis of KCC-1 and γ-Fe_2O_3/KCC-1. The surface area (*SA*) and pore volume (V_p) of synthesized magnetic γ-Fe_2O_3/KCC-1 were slightly lower (*SA* = 401 $m^2\ g^{-1}$, V_p = 0.90 $cm^3\ g^{-1}$) compared to the KCC-1 (*SA* = 588 $m^2\ g^{-1}$, V_p = 1.28 $cm^3\ g^{-1}$). These findings indicated the successful doping of Fe within the pore channels of KCC-1. Similar observations were obtained in the study of Zhang et al. [20] for the preparation of magnetic Fe-SBA-15. In their research, the value of *SA* reduced from 524 $m^2\ g^{-1}$ to 308 $m^2\ g^{-1}$, and pore size from 72.8 Å to 72.6 Å.

Table 1. BET analysis results of KCC-1 and γ-Fe_2O_3/KCC-1

Sample	Surface Area, SA (m^2 g^{-1})	Total pore volume, V_p (cm^3 g^{-1})
KCC-1	588	1.28
γ-Fe_2O_3/KCC-1	401	0.90

Figure 1 showed the TEM images for magnetic γ-Fe_2O_3/KCC-1 with deep black crystal portions, indicating a successful impregnation of magnetic γ-Fe_2O_3/KCC-1. The introduction of magnetic γ-Fe_2O_3 was able to maintain uniform spheres with the fibrous morphology of KCC-1. A similar study by Zhang et al. [20] on the preparation of magnetic Fe-SBA-15 also showed that the addition of Fe was able to retain the SBA-15 uniformity of mesopore.

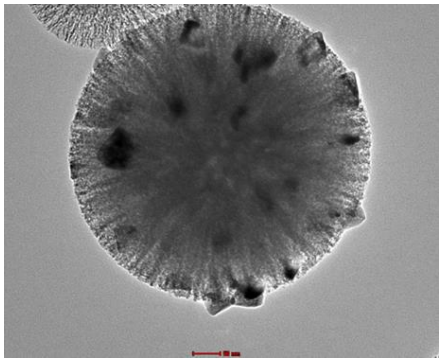

Figure 1. TEM images for magnetic γ-Fe_2O_3/KCC-1 with deep black crystal portions indicate the iron metal particles.

Response Surface Methodology

Table 2 tabulates the experimental design and corresponding response. The regression coefficient analysis was performed, and the quadratic model of Pb(II) elimination onto magnetic γ-Fe_2O_3/KCC-1 in terms of coded forms were described by Equation (3).

Table 2. Design of experiments and experimental response for Pb(II) removal by magnetic γ-Fe_2O_3/KCC-1

Run	Manipulated Variables						Response
	Initial Concentration (mg/L), X_1		Adsorbent Dosage (g/L), X_2		Initial pH, X_3		Pb(II) removal, Y (%)
	Uncoded	Coded	Uncoded	Coded	Uncoded	Coded	
1	50	-1	0.5	-1	2	-1	83.19
2	50	-1	0.5	-1	10	1	86.18
3	50	-1	5	1	2	-1	81.67
4	50	-1	5	1	10	1	84.91
5	400	1	0.5	-1	2	-1	87.82
6	400	1	0.5	-1	10	1	86.75
7	400	1	5	1	2	-1	86.63
8	400	1	5	1	10	1	85.42
9	50	-1	2.75	0	6	0	85.19
10	400	1	2.75	0	6	0	89.78
11	225	0	0.5	-1	6	0	87.49
12	225	0	5	1	6	0	86.77
13	225	0	2.75	0	2	-1	88.74
14	225	0	2.75	0	10	1	88.70
15	225	0	2.75	0	6	0	90.82
16	225	0	2.75	0	6	0	90.49

$$Y = 78.46239 + 0.04414X_1 + 2.05134X_2 + 0.86374X_3 - 0.00006X_1^2 - 0.42687X_2^2 - 0.03569X_3^2 + 0.00009X_1X_2 - 0.00152X_1X_3 + 0.00153X_2X_3 \quad (3)$$

Where Y is the predicted percentage removal of Pb(II), X_1 is the initial Pb(II) concentration, X_2 is the adsorbent dosage, and X_3 is the initial pH.

Analysis of variance (ANOVA) was employed to investigate the statistical and adequacy of the quadratic model. It is a statistical method of comparing the experimental means of two or more groups, in which the significance of the coefficient was decided by the *F*-value and *p*-value. The corresponding coefficients are more meaningful when the *F*-value is larger and the *p*-value is smaller. The greater calculated *F*-value (F_{model} = 11.73008) than that of the tabulated *F*-value (F_{table} = 4.0990) at the 5% significance level indicates that the model was highly significant, as noted in the data in Table 3. These results showed that the quadratic model obtained from Eq. 3 provides a good prediction at a 5% level of significance.

Table 1. ANOVA analysis results of Pb(II) removal by magnetic γ-Fe_2O_3/KCC-1

Sources	Sum of Squares (SS)	Degree of freedom (d.f)	Mean Square (MS)	*F*-value	$F_{0.05}$
Regression (SSR)	90.07079	9	10.00787	11.73008	>4.0990
Residual	5.11910	6	0.85318		
Total (SST)	95.18989	15			

Figure 2 demonstrates the parity plot that compares the actual values and predicted values of percentage Pb(II) removal by magnetic γ-Fe_2O_3/KCC-1 with the determination coefficient, R^2 of 0.9462. Based on this result, it can be deduced that the model is responsible for 94.6 % of the variability found in the data. According to Asfaram et al. [21], the value of R^2 must be in the range of 0.8 – 1.0 for a better correlation of a model. Therefore, the R^2 value (0.9462) given by the RSM software provided that the quadratic model had a good relationship between the predicted and experimental values.

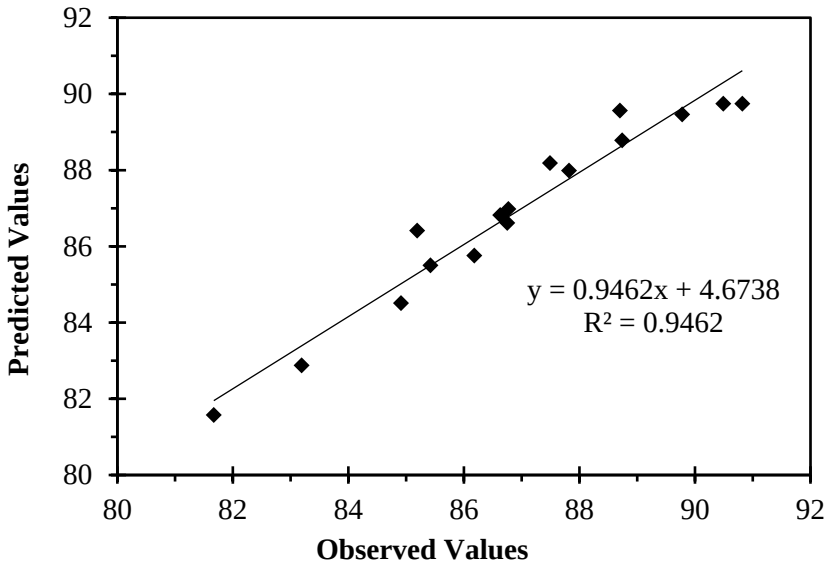

Figure 2. Parity plot of the observed and predicted percentage removal of Pb(II) removal by magnetic γ-Fe_2O_3/KCC-1.

Figure 3 displays the pareto chart and corresponding *p*-values of percentage removal of Pb(II). To study the significance of each respective coefficient, *p*-value and *t*-value was utilized whereby the coefficient with the smallest *p*-value or the largest *t*-value corresponds to the most significant variable [10]. As demonstrated in Figure 3, the linear term of initial Pb(II) concentration (X_1), quadratic term of adsorbent dosage (X_2^2), combination linear term of initial Pb(II) concentration associated with initial pH (X_1X_3), quadratic term of initial Pb(II) concentration (X_1^2), and linear term of adsorbent dosage (X_2) were considered as statistically significant aspects. The remaining factor terms may be regarded as less significant since they consist of a larger *p*-value (p>0.05). Notably, the linear term of initial Pb(II) concentration (X_1) had the largest effect on the percentage removal of Pb(II) as it had the smallest *p*-value (0.0031) and the largest *t*-value (5.2243) compared to other variable terms.

The initial concentration of Pb(II) is one of the most crucial variables because it influences how much mass is transferred from the liquid phase to the solid phase [22]. Interestingly, at low Pb(II) initial concentration, the ratio of active surface sites of the adsorbent to the total initial Pb(II) ions in the solution is relatively high. Consequently, all Pb(II)

ions in the solvent can engage with the active sites of the adsorbent and be separated from the solution [23]. Similar findings were also described in the literature [24-25]. Based on the study by Chen et al. [24] for the adsorption of Pb(II) onto fallen *Cinnamomum camphora* leaves (FCCL), the kinetic study revealed Pb(II) was mainly controlled by the initial Pb(II) concentration. From the study, the equilibrium adsorption capacity increased with increasing initial Pb(II) concentration. This resulted in a strong driving force of mass transport that was induced by the presence of an elevated concentration of Pb(II). This result is also supported by another study from Kalantari et al. [25] on Pb(II) ion adsorption from aqueous solution onto Fe_3O_4/Talc nanocomposite, where the effect of three independent variables (initial Pb(II) concentration, adsorbent dosage, and removal time) were investigated, and the initial Pb(II) concentration was the most critical factor compared to adsorbent dosage and removal time.

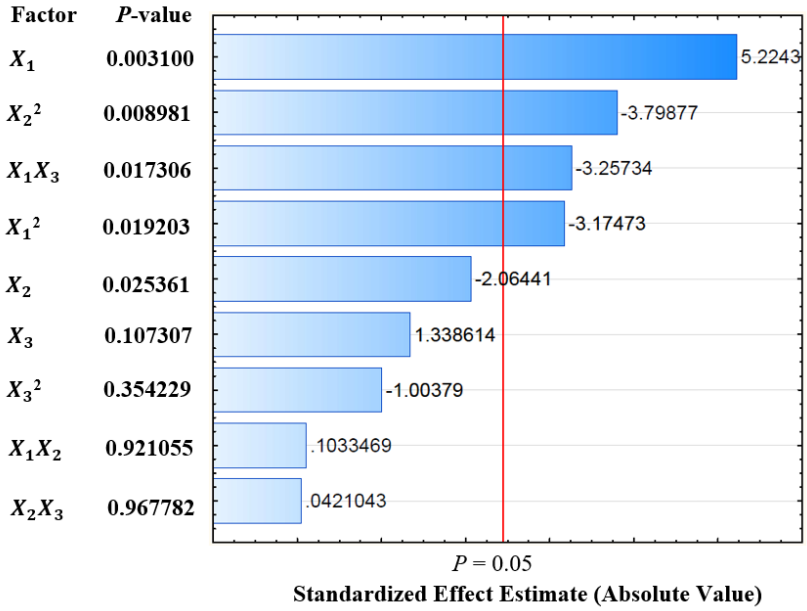

Figure 3. Pareto chart and p-values of percentage removal of Pb(II) removal by magnetic γ-Fe_2O_3/KCC-1.

Figure 4(A) depicts the simultaneous effects of Pb(II) initial concentration (X_1) and adsorbent dosage (X_2) on the percentage of Pb(II) removal. Initial Pb(II) concentration had a stronger influence on the response surface than adsorbent dose, as shown by the Pareto chart in Figure 3, which revealed a smaller *p*-value for initial Pb(II) concentration (0.0031) than adsorbent dosage (0.025361). As depicted in Figure 4(A), the degradation rate of Pb(II) improved with increasing initial Pb(II) concentration and catalyst loading till it achieved an optimum at X_1= 260-340 mg/L and X_2= 2-3 g/L, but then decreased at a higher value. As for the contribution of the initial Pb(II) concentration, the higher the initial Pb(II) concentration contributes to a stronger driving force of Pb(II) ions towards the active sites of magnetic γ-Fe_2O_3/KCC-1, as well as boosting the concentration gradient and hence improved the Pb(II) removal, which in line with the literature [26]. Initially, the Pb(II) adsorption capacity immediately improves with an increment in the initial concentration of Pb(II). The Pb(II) ions attach themselves to the plentiful adsorption sites on the adsorbent's surface, which leads to a higher absorptivity of the adsorbent. This is due to the adsorbent's large surface area, resulting in a higher number of active sites for the sorption process. However, there is a slight decrease in Pb(II) removal upon further elevating the initial Pb(II) concentration. That is because the binding sites have become saturated with adsorbed Pb(II) ions, as the emergence of a greater concentration of Pb(II) may minimize the amount of Pb(II) that can be absorbed by the adsorbent. Regarding the impact of the adsorbent dosage, it is possible to claim that the rise in Pb(II) removal at the start was caused by a larger supply of accessible binding sites on the adsorbate. However, increasing the adsorbent dosage until a higher value will result in a slower rate of adsorption in the final step. This could be because at smaller doses, all active sites were exposed, whereas, at larger dose levels, only a small amount of the active sites were made accessible [18]. Therefore, a higher adsorbent dose may promote aggregation, which will result in decreasing the adsorbent's surface area and, ultimately, reduce the amount of Pb(II) that is absorbed by the adsorbent. The significant impact of the initial concentration of Pb(II) and the amount of adsorbent used on Pb(II) removal was also reported by Javabakht & Ghoreishi [27] using CPL/Fe_3O_4 nanocomposite. The research stated that a rise in the initial concentration of Pb(II) led to an increase in the removal of Pb(II) since the concentration gradient's driving force was stronger. Similar behaviour also can be observed for the removal of Pb(II) from an aqueous solution by *Hypnea valentiae* [26]. The authors claimed that the removal of Pb(II) increased with an increase in adsorbent dosage up to 5 g/L and decreased after that. Therefore, the optimum value of the adsorbent dosage was found to be 5 $\pm$ 0.2 g/L which is close enough to this study's result of the adsorbent dosage is 2-3 g/L. The same phenomena were also reported in the literature [21,28] for Pb(II) removal onto modified activated carbon (Mn-Fe_3O_4-NP_S-AC) and modified chitosan (MCMC-PEI), respectively.

Figure 4(B) depicted the subsequent impact of initial Pb(II) concentration (X_1) and pH (X_3) on Pb(II) removal. From the analysis of the response surface plot, both effects show a high increment potential when their respective value increases and give a high value of percentage removal. Even though pH had a negligible impact on the response surface, the initial Pb(II) concentration greatly impacted the response curve. This was proved by the Pareto chart (Figure 3), which showed a smaller *p*-value of initial Pb(II) concentration (0.0031) as compared to the pH (0.107307). As illustrated in Figure 4(B), the increase in both initial Pb(II) concentration and pH resulted in a simultaneously increasing trend in Pb(II) removal, with initial Pb(II) concentration showing the highest increment compared to pH. The highest efficacy of Pb(II) removal was obtained at a pH between 4-7 and an initial Pb(II) concentration of 270-350 mg/L. The pH could affect the metal-binding sites of adsorbent and functional groups of Pb(II) in solution [29]. At a lower pH (<4.0), the protons (H^+ions) become competitive with Pb(II) for the exchangeable cations on the adsorbent surface. More protons (H^+ions) were binding on the surface of the adsorbent surface compared to Pb(II) ions, resulting in lower adsorption of Pb(II). Due to the lesser competitive protons (H^+ions) on the adsorbent surface, more exchangeable cations can be transferred with Pb(II) as the pH rises, resulting in a rapid increase in Pb(II) adsorption. There is a slight decrease in the adsorption of Pb(II) at higher pH value (>10) and higher initial Pb(II) concentration (> 400 mg/L) due to the formation of soluble hydroxyl complexes such as $Pb(OH^+)$ and/or $Pb(OH)_2$ [18]. A similar finding on the effects of initial Pb(II) concentration and pH on Pb(II) elimination was also studied by Sahan & Ozturk [23] using pumice as an adsorbent on Pb(II) removal. Based on their results, raising the pH of Pb(II) solution from 5.50 to 5.80 increased the adsorption capacity sharply. The adsorption capacity decreases with increasing pH as the negative charge density on the adsorbent's surface increases due to deprotonation of the metal-binding sites. Javanbakht et al. [30] also reported the same findings on Pb(II) removal by magnetic chitosan/clinoptilolite/magnetite nanocomposite, and the highest Pb(II) removal was gained at the initial Pb(II) concentration of 90 mg/g and pH 6.

Figure 4(C) illustrates the simultaneous outcomes of adsorbent dosage (X_2) and pH (X_3) on Pb(II) elimination. An increase in adsorbent dosage and pH consequently increase the Pb(II) removal, achieving optimal (X_2 = 1-4 g/L and X_3 = 2.5-10), and reduced at raised adsorbent dosage. As the adsorbent dosage increased, the surface area and adsorption sites for the adsorbent increased rapidly, resulting in high adsorption of Pb(II). However, at a specific adsorbent dosage with high availability of adsorbent, the solution becomes unsaturated, resulting in lower adsorption of Pb(II). Another reason may arise because of the agglomeration of adsorbent at a high dosage [27]. Similar comments were made by Khazaei et al. [31] on Pb(II) removal using Fe_3O_4@SiO_2-GO as an adsorbent. The authors concluded that the maximum Pb(II) was obtained with a pH of 6.5 to 8.5, and Pb(II) removal was significantly influenced by pH and adsorbent dosage. Javanbakht et al. [30] also reported the same results using chitosan/clinoptilolite/magnetite nanocomposite to eliminate Pb(II) ions from an aqueous solution. The researchers determined that with a high adsorbent dosage, the overall surface area of the adsorbent decreased while the diffusional path length increased. At higher adsorbent concentrations, the particles may desorb some of the loosely bound Pb(II) ions from the adsorbent surface, decreasing Pb(II) elimination.

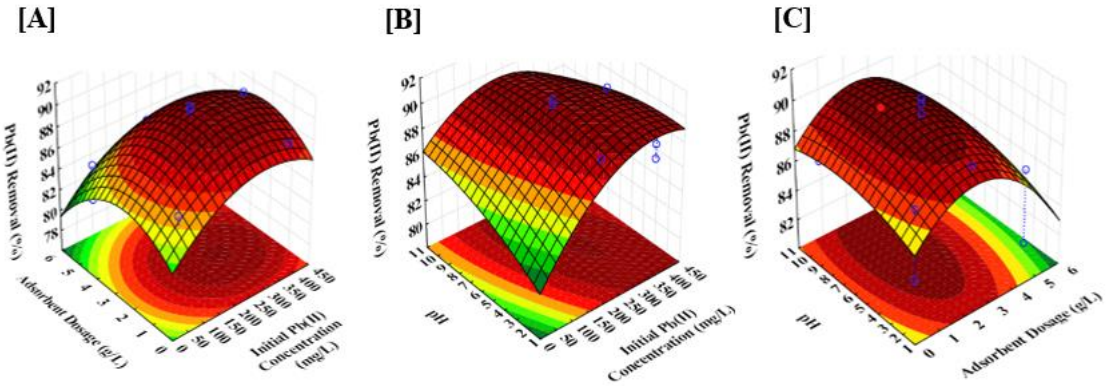

Figure 4. The 3D surface plots showing the influences of (A) Initial Pb(II) concentration and adsorbent dosage; (B) Initial Pb(II) concentration and pH; (C) Adsorbent dosage and pH.

Optimization

Based on the RSM study, at an initial Pb(II) concentration of 302.37 mg/L, the adsorbent dosage of 2.44 g/L, and pH of 5.7, the predicted optimal percentage of Pb(II) removal obtained was 90.11 %. Therefore, an extra experiment was conducted in triplicate under optimal conditions to confirm the validity of the optimization result obtained by the response surface analysis. The average percentage of Pb(II) removal in those three adsorption experiments was 91%. The percentage error between predicted and actual responses is 0.99 % (Table 4), which is acceptable because it is less than 5%.

Table 2. Percentage error between the predicted and observed responses at the optimal conditions.

	Predicted value (%)	Observed value (%)	Error (%)
Percentage Removal	90.11	91.00	0.99

Table 5 compares the adsorption capacity of various mesoporous silica adsorbents for Pb(II) removal reported in the literature. The magnetic γ-Fe_2O_3/KCC-1 has a higher adsorption capacity which was 91%, compared to KCC-1 (83%). An increase in Pb(II) removal using magnetic γ-Fe_2O_3/KCC-1 compared to KCC-1 indicates that Fe_2O_3 was able to increase the adsorbent's physicochemical qualities (high surface area and well distribution of active sites), hence increasing its adsorption capacity [32]. Moreover, magnetic γ-Fe_2O_3/KCC-1 was found to have a comparable adsorption capacity compared to other adsorbents. It is interesting to note that although dendrimer amine grafted mesoporous silica [33], metformin amino-substituted SBA-15 magnetic nanocomposite [34], S_4 functionalized mesoporous silica nanospheres (MSCMNPs- S_4) [35], magnetic silica–xanthan gum composites [36] have comparable adsorption capacity with magnetic γ-Fe_2O_3/KCC-1; however, magnetic γ-Fe_2O_3/KCC-1 has advantages in cost factor because this adsorbent was prepared from POFA waste.

Table 3. Comparison of magnetic γ-Fe_2O_3/KCC-1 with literature for Pb(II) removal.

Adsorbent	Pb(II) Removal (%)	Reference
Magnetic γ-Fe_2O_3/KCC-1	91.00	This study
KCC-1	83.00	This study
Dendrimer amine grafted mesoporous silica	95.00	[33]
Metformin amino-substituted SBA-15 magnetic nanocomposite	96.00	[34]
S_4 functionalized mesoporous silica nanospheres (MSCMNPs- S_4)	95.70	[35]
MWCNT-Fe_3O_4	90.20	[37]
Magnetic silica–xanthan gum composites	93.77	[36]
o-Vanillin functionalized mesoporous silica-coated magnetite nanoparticles	90.00	[38]

CONCLUSION

The magnetic γ-Fe_2O_3/KCC-1 prepared from POFA is considered an excellent and low-cost adsorbent for the Pb(II) removal from an aqueous solution. The characterization of magnetic γ-Fe_2O_3/KCC-1 confirmed a successful impregnation of γ-Fe_2O_3 onto KCC-1. The optimization by RSM with independent variables of initial Pb(II) concentration (X_1), γ-Fe_2O_3/KCC-1 dosage (X_2), and initial pH (X_3) revealed that the optimum conditions were found at X_1 = 302.37 mg/L, X_2 = 2.44 g/L, and X_3 = 7 pH. The highest percentage removal of Pb(II) obtained at optimum conditions were 90.11% predictably and 91% experimentally, with an error of only 0.99% based on the difference between predicted and experimental values. Based on ANOVA, the most contributed factor was initial Pb(II) concentration (X_1). The magnetic γ-Fe_2O_3/KCC-1 not only has good adsorption but also can be conveniently extracted from the solution due to its magnetic properties. Therefore, this research affirmed that magnetic γ-Fe_2O_3/KCC-1 has a great potential as an adsorbent for Pb(II) removal from aqueous solutions with a percentage removal of 91% and adsorption capacity of 112.77 mg/g.

ACKNOWLEDGEMENT

The financial assistance by Universiti Malaysia Pahang through research grant RDU1903130 and RDU1803184 are acknowledged.

REFERENCES

[1] X. Yang, G. Xu, and H. Yu, "Removal of lead from aqueous solutions by ferric activated sludge-based adsorbent derived from biological sludge," *Arabian Journal of Chemistry*, vol. 12, no. 8, pp. 4142–4149, Dec. 2019, doi: 10.1016/j.arabjc.2016.04.017.

[2] US EPA, "Basic Information about Lead Air Pollution _ Lead (Pb) Air Pollution _ US EPA," 2017.

[3] R. Emily, "Lead - Element information, properties and uses | Periodic Table," *Royal Society of Chemistry*, 2014.

[4] C. Q. Teong, H. D. Setiabudi, N. A. S. El-Arish, M. B. Bahari, and L. P. Teh, "Vatica rassak wood waste-derived activated carbon for effective Pb(II) adsorption: Kinetic, isotherm and reusability studies," *Materials Today: Proceedings*, vol. 42, pp. 165–171, 2019, doi: 10.1016/j.matpr.2020.11.270.

[5] S. Y. Kang, J. U. Lee, S. H. Moon, and K. W. Kim, "Competitive adsorption characteristics of Co^{2+}, Ni^{2+}, and Cr^{3+} by IRN-77 cation exchange resin in synthesized wastewater," *Chemosphere*, vol. 56, no. 2, pp. 141–147, Jul. 2004, doi: 10.1016/j.chemosphere.2004.02.004.

[6] Y. Ku and I. L. Jung, "Photocatalytic reduction of Cr(VI) in aqueous solutions by UV irradiation with the presence of titanium dioxide," *Water Research*, vol. 35, no. 1, pp. 135–142, 2001, doi: 10.1016/S0043-1354(00)00098-1.

[7] Y. Feng, L. Yang, J. Liu, and B. E. Logan, "Electrochemical technologies for wastewater treatment and resource reclamation," *Environmental Science: Water Research and Technology*, vol. 2, no. 5. Royal Society of Chemistry, pp. 800–831, Sep. 2016. doi: 10.1039/c5ew00289c.

[8] A. J. Hargreaves *et al.*, "Impacts of coagulation-flocculation treatment on the size distribution and bioavailability of trace metals (Cu, Pb, Ni, Zn) in municipal wastewater," *Water Research*, vol. 128, pp. 120–128, Jan. 2018, doi: 10.1016/j.watres.2017.10.050.

[9] M. İnce and O. Kaplan İnce, "An Overview of Adsorption Technique for Heavy Metal Removal from Water/Wastewater: A Critical Review," *International Journal of Pure and Applied Sciences*, pp. 10–19, Dec. 2017, doi: 10.29132/ijpas.372335.

[10] R. Hasan and H. D. Setiabudi, "Removal of Pb(II) from aqueous solution using KCC-1: Optimization by response surface methodology (RSM)," *Journal of King Saud University - Science*, vol. 31, no. 4, pp. 1182–1188, 2019, doi: 10.1016/J.JKSUS.2018.10.005.

[11] V. Polshettiwar, D. Cha, X. Zhang, and J. M. Basset, "High-surface-area silica nanospheres (KCC-1) with a fibrous morphology," *Angewandte Chemie - International Edition*, vol. 49, no. 50, pp. 9652–9656, Dec. 2010, doi: 10.1002/anie.201003451.

[12] R. Hasan, C. C. Chong, S. N. Bukhari, R. Jusoh, and H. D. Setiabudi, "Effective removal of Pb(II) by low-cost fibrous silica KCC-1 synthesized from silica-rich rice husk ash," *Journal of Industrial and Engineering Chemistry*, vol. 75, pp. 262–270, Jul. 2019, doi: 10.1016/J.JIEC.2019.03.034.

[13] C. C. Chong, N. Abdullah, S. N. Bukhari, N. Ainirazali, L. P. Teh, and H. D. Setiabudi, "Hydrogen production via CO2 reforming of CH4 over low-cost Ni/SBA-15 from silica-rich palm oil fuel ash (POFA) waste," *International Journal of Hydrogen Energy*, vol. 44, no. 37, pp. 20815–20825, Aug. 2019, doi: 10.1016/J.IJHYDENE.2018.06.169.

[14] V. Ranjithkumar, S. Sangeetha, and S. Vairam, "Synthesis of magnetic activated carbon/α-Fe2O3 nanocomposite and its application in the removal of acid yellow 17 dye from water," *Journal of Hazardous Materials*, vol. 273, pp. 127–135, May 2014, doi: 10.1016/j.jhazmat.2014.03.034.

[15] Y. Zou, J. Kan, and Y. Wang, "Fe_2O_3-Graphene rice-on-sheet nanocomposite for high and fast lithium ion storage," *Journal of Physical Chemistry C*, vol. 115, no. 42, pp. 20747–20753, Oct. 2011, doi: 10.1021/jp206876t.

[16] S. Azizi, N. Shadjou, and M. Hasanzadeh, "KCC-1 aminopropyl-functionalized supported on iron oxide magnetic nanoparticles as a novel magnetic nanocatalyst for the green and efficient synthesis of sulfonamide derivatives," *Applied Organometallic Chemistry*, vol. 34, no. 1, p. e5321, 2020, doi: 10.1002/AOC.5321.

[17] J. Wang, X. Shao, Q. Zhang, J. Ma, and H. Ge, "Preparation and photocatalytic application of magnetic Fe2O3/SBA-15 nanomaterials," *Journal of Molecular Liquids*, vol. 260, pp. 304–312, Jun. 2018, doi: 10.1016/j.molliq.2018.03.109.

[18] A. A. Alghamdi, A. B. Al-Odayni, W. S. Saeed, A. Al-Kahtani, F. A. Alharthi, and T. Aouak, "Efficient adsorption of lead (II) from aqueous phase solutions using polypyrrole-based activated carbon," *Materials*, vol. 12, no. 12, Jun. 2019, doi: 10.3390/ma12122020.

[19] N. Atiqah and H. D. Setiabudi, "Synthesis And Characterization Of Kcc-1 From Palm Oil Fuel Ash (Pofa) For Lead Removal," *Universiti Malaysia Pahang, Gambang*, vol. 60, pp. 24–27, 2018.

[20] H. Zhang, H. Huang, Y. Ji, Z. Qiao, C. Zhao, and J. He, "Preparation, characterization, and application of magnetic Fe-SBA-15 mesoporous silica molecular sieves," *Journal of Automated Methods and Management in Chemistry*, vol. 2010, 2010, doi: 10.1155/2010/323509.

[21] A. Asfaram, M. Ghaedi, A. Goudarzi, and M. Rajabi, "Response surface methodology approach for optimization of simultaneous dye and metal ion ultrasound-assisted adsorption onto Mn doped Fe3O4-NPs loaded on AC: Kinetic and isothermal studies," *Dalton Transactions*, vol. 44, no. 33, pp. 14707–14723, Jul. 2015, doi: 10.1039/c5dt01504a.

[22] R. Singh and R. Bhateria, "Optimization and Experimental Design of the Pb^{2+}Adsorption Process on a Nano-Fe3O4-Based Adsorbent Using the Response Surface Methodology," *ACS Omega*, Nov. 2020, doi: 10.1021/acsomega.0c04284.

[23] T. Şahan and D. Öztürk, "Investigation of Pb(II) adsorption onto pumice samples: Application of optimization method based on fractional factorial design and response surface methodology," *Clean Technologies and Environmental Policy*, vol. 16, no. 5, pp. 819–831, Sep. 2014, doi: 10.1007/s10098-013-0673-8.

[24] H. Chen, J. Zhao, G. Dai, J. Wu, and H. Yan, "Adsorption characteristics of Pb(II) from aqueous solution onto a natural biosorbent, fallen Cinnamomum camphora leaves," *Desalination*, vol. 262, no. 1–3, pp. 174–182, Nov. 2010, doi: 10.1016/j.desal.2010.06.006.

[25] K. Kalantari, M. B. Ahmad, H. R. F. Masoumi, K. Shameli, M. Basri, and R. Khandanlou, "Rapid adsorption of heavy metals by Fe3O4/talc nanocomposite and optimization study using response surface methodology," *International Journal of Molecular Sciences*, vol. 15, no. 7, pp. 12913–12927, Jul. 2014, doi: 10.3390/ijms150712913.

[26] M. Rajasimman and K. Murugaiyan, "Application of the statistical design for the sorption of lead by Hypnea valentiae," *Journal of Advanced Chemical Engineering*, vol. 2, pp. 1–7, 2012, doi: 10.4303/jace/A110402.

[27] V. Javanbakht and S. M. Ghoreishi, "Application of response surface methodology for optimization of lead removal from an aqueous solution by a novel superparamagnetic nanocomposite," *Adsorption Science and Technology*, vol. 35, no. 1–2, pp. 241–260, Mar. 2017, doi: 10.1177/0263617416674474.

[28] Y. Wang *et al.*, "Rapid removal of Pb(II) from aqueous solution using branched polyethylenimine enhanced magnetic carboxymethyl chitosan optimized with response surface methodology," *Scientific Reports*, vol. 7, no. 1, Dec. 2017, doi: 10.1038/s41598-017-09700-5.

[29] W. S. Wan Ngah, L. C. Teong, and M. A. K. M. Hanafiah, "Adsorption of dyes and heavy metal ions by chitosan composites: A review," *Carbohydrate Polymers*, vol. 83, no. 4. pp. 1446–1456, Feb. 2011. doi: 10.1016/j.carbpol.2010.11.004.

[30] V. Javanbakht, S. M. Ghoreishi, N. Habibi, and M. Javanbakht, "A novel magnetic chitosan/clinoptilolite/magnetite nanocomposite for highly efficient removal of Pb(II) ions from aqueous solution," *Powder Technology*, vol. 302, pp. 372–383, Nov. 2016, doi: 10.1016/j.powtec.2016.08.069.

[31] M. Khazaei *et al.*, "Response surface modeling of lead (II) removal by graphene oxide-Fe_3O_4 nanocomposite using central composite design," *Journal of Environmental Health Science and Engineering*, vol. 14, no. 1, pp. 1–14, Jan. 2016, doi: 10.1186/s40201-016-0243-1.

[32] S. M. Reda, S. M. AL-Ghannam, and S. N. A. El-Rahman, "Effect of source of silica on properties of Fe2O3/SiO2 nanocompsites and their application on hepatic injury in rats as adsorbents for removal of heavy metal from drinking water," *Asian Journal of Chemistry*, vol. 30, no. 3, pp. 625–632, 2018, doi: 10.14233/ajchem.2018.21062.

[33] A. Shahbazi, H. Younesi, and A. Badiei, "Functionalized SBA-15 mesoporous silica by melamine-based dendrimer amines for adsorptive characteristics of Pb(II), Cu(II) and Cd(II) heavy metal ions in batch and fixed bed column," *Chemical Engineering Journal*, vol. 168, no. 2, pp. 505–518, Apr. 2011, doi: 10.1016/j.cej.2010.11.053.

[34] S. Shahabuddin "Kinetic and equilibrium adsorption of lead from water using magnetic metformin-substituted SBA-15," *Environmental Science: Water Research and Technology*, vol. 4, no. 4, pp. 549–558, Apr. 2018, doi: 10.1039/c7ew00552k.

[35] H. Vojoudi, A. Badiei, S. Bahar, G. Mohammadi Ziarani, F. Faridbod, and M. R. Ganjali, "A new nano-sorbent for fast and efficient removal of heavy metals from aqueous solutions based on modification of magnetic mesoporous silica nanospheres," *Journal of Magnetism and Magnetic Materials*, vol. 441, pp. 193–203, Nov. 2017, doi: 10.1016/j.jmmm.2017.05.065.

[36] X. Peng *et al.*, "Magnetic Fe_3O_4 @ silica-xanthan gum composites for aqueous removal and recovery of Pb^{2+}," *Colloids and Surfaces A: Physicochemical and Engineering Aspects*, vol. 443, pp. 27–36, Feb. 2014, doi: 10.1016/j.colsurfa.2013.10.062.

[37] G. Milad and F. Hossein, "Response surface methodology optimization of cobalt (II) and lead (II) removal from aqueous solution using MWCNT-Fe_3O_4 nanocomposite," *Iranian Journal of Chemistry and Chemical Engineering*, vol. 36, no. 5, pp. 129–141, 2017.

[38] D. C. Culita, C. M. Simonescu, R. E. Patescu, M. Dragne, N. Stanica, and O. Oprea, "o-Vanillin functionalized mesoporous silica - coated magnetite nanoparticles for efficient removal of Pb(II) from water," *Journal of Solid State Chemistry*, vol. 238, pp. 311–320, Jun. 2016, doi: 10.1016/j.jssc.2016.04.003.